

Variable Perturbation Based Fault Diagnosis in Industrial Processes

Tanmaya Singhal¹, Kuldeep Singh², Kalyani Zope³, Sri Harsha Nistala⁴ and Venkataramana Runkana⁵

^{1,2,3,4,5}TCS Research, Tata Consultancy Services Ltd., Pune – 411013, India

tanmaya.singhal@tcs.com

kuldeep.s5@tcs.com

kalyani.zope@tcs.com

sriharsha.nistala@tcs.com

venkat.runkana@tcs.com

ABSTRACT

Real-time fault detection, classification and diagnosis in manufacturing and process industries is essential to prevent unplanned downtime and improve the reliability of industrial operations. While several well-accepted machine learning techniques exist for fault detection and classification, there is a need for a reliable and generalized fault diagnosis technique that identifies sensors responsible for industrial faults in real time. In this work, we propose a variable perturbation matrix-based method for fault diagnosis in industrial processes. We utilize the Long Short-Term Memory for prediction due to its ability to memorize temporal information in time-series data. First, the fault is detected, then one or more independent variables are perturbed across the fault detection point to check the sensitivity of the diagnosis model for the corresponding variables. Thus, a perturbation matrix is calculated and variables with high sensitivity are selected as the variables responsible for fault. The proposed method is applied to an Industry 4.0 quality control test bed set up for electronic components, the dataset for which is provided in the Prognostics and Health Management Euorpe-21 (PHME-21) data challenge. The proposed method accurately detected and classified 6 faults in the test bed and correctly diagnosed the most significant variables. Due to high fault detection accuracy coupled with sensitivity-based fault diagnosis, the method is suitable for multivariate industrial systems.

Keywords: Fault classification, Fault localization, Predictive maintenance, Artificial Intelligence, Manufacturing Industry

1. INTRODUCTION

The rise of Industry 4.0 has transformed manufacturing and process industries and equipped industrial processes with a large number of sensors leading to the availability of huge amounts of sensor data in real-time. This data contains valuable information about the state of health of the operation and equipment and is of immense value to plant

personnel for effective process monitoring and control, process optimization, and predictive maintenance for maintaining and improving the plant KPIs such as efficiency, productivity, product quality, reliability, etc. For predictive maintenance, a robust fault detection and diagnosis (FDD) solution is a key requirement from industries as unaddressed faults can hamper normal operation and lead to unplanned downtime, material loss, adverse impact to equipment, deterioration of product quality, and ultimately loss of revenue. While fault detection comprises monitoring the process or equipment for anomalous behavior, fault diagnosis typically entails classification of the detected fault into one or more known fault classes, identifying the most significant variables bearing the fault signature (fault localization/isolation) and root cause identification.

Most FDD methods use process models or data-driven models for detecting and diagnosing faults. Process model-based methods utilize mathematical models of the system and work quite well for linear systems (Fagarasan & Iliescu, 2008). Data-driven methods, on the other hand, do not require mechanistic models but use historical process data to build the models. Techniques such as principal component analysis (PCA), partial least squares (PLS) and many extensions of these two techniques have been widely used for building data-driven models for detection and diagnosis of faults in multivariate data (Lee, Han, & Yoon, 2004; Zhang & Qin, 2010). These methods can handle a large number of highly correlated variables and reduce the high-dimensional variable space into a low-dimensional latent space. However, these techniques fail to capture spatial and/or temporal correlations among the process variables which affects the fault diagnosis performance. To address this shortcoming, probabilistic, machine learning and deep learning techniques have been used. A detailed review of such data-driven methods is provided by Zhang, Yang, and Wang (2019). For example, Li, Wei, Wang, and Zhou (2017) used Hidden Markov models for fault detection and classification in rotating machinery. Khoukhi and Khalid

(2015) evaluated the efficacy of hybrid data-driven techniques that use fuzzy logic combined with neural networks for fault detection and isolation.

More recently, Park, Marco, Shin, and Bang (2019) proposed an integrated semi-supervised learning approach for fault detection and classification of rare events in multivariate time series data by combining an autoencoder for detection and a long short-term memory (LSTM) network for classification. Long, Mou, Zhang, Zhang and Li (2021) utilized a sparse auto-encoder and support vector machine based deep hybrid learning approach for intelligent fault diagnosis of multi-joint industrial robots while Kim, Cho, Lee and Cho (2019) used a self-attentive convolutional neural network for FDD of variable length sensor data in semiconductor manufacturing. Belagoune, Bali, Bakdi, Baadji and Atif (2021) performed deep recurrent neural network-based fault region identification, fault classification and fault location prediction in Two-Area Four-Machine Power Systems. Cho, Choi, Gao and Moan (2021) employed Kalman filter with artificial neural networks for fault diagnosis of a spar floating wind turbine with variable wind and wave conditions. Michau, Palm and Fink (2017) used a stacked auto-encoder to learn the underlying features of the data and a one-class classifier for detecting power plant generator interturn failures and isolating the most deviating signal components. Aydemir, Avci, Kocakulak and Bekiryazici (2021) employed ensemble of binary LSTM classifiers for fault detection and root cause variable identification in quality-control systems with multiple subsystems.

While a multitude of techniques are available for fault detection and classification, there are limited approaches for fault localization and root cause identification, probably due to the challenges associated with modeling the nonlinear interactions among process variables and capturing the nonstationary behavior that is typical of most industrial processes. It is, however, crucial to have a reliable and generalized fault localization technique that could identify the sensors responsible for industrial faults in real-time. For this, a variable perturbation matrix-based method for fault localization is proposed in this work. The variable perturbation matrix (VPM) is obtained by perturbing one or more sensor variables across the fault detection point. For every variable, the cumulative perturbation score is computed by measuring the sensitivity of variables to a data-driven diagnosis model. The variables with the highest perturbation scores are selected as the variables responsible for the fault. The proposed fault localization approach is demonstrated on a quality control and assurance test setup used for fuse testing in the manufacturing industry. The key contributions of this work are:

- A dynamic sensitivity-based robust fault localization approach that works for systems with nonlinear behavior and interacting variables

- A perturbation score corresponding to each variable for the detected fault signifying the importance and ranking of the identified variables
- The utility of the approach is demonstrated on an industrial test bed and found to have an average diagnosis accuracy of ~70%

The paper is structured as follows. Section 2 describes the proposed method for fault detection and diagnosis. The fuse test bed on which the proposed approach is demonstrated is described in Section 3. Development of detection and diagnosis models is presented in Section 4. The results of the study are discussed in Section 5. Finally, the conclusions and future work are presented in Section 6.

2. PROPOSED METHODOLOGY

The proposed methodology for fault diagnosis, specifically fault localization comprises modules for fault detection and classification and identification of the most significant variable/s via variable perturbation as shown in Figure 1. Sensor data from an industrial system is fetched by the fault detection and classification module in real-time which utilizes fault detection and classification model(s) to detect any faulty operation. If no fault is detected, the fault detection step is repeated on the next window of sensor data without raising any alarms or notifications. If faulty operation is detected, the module analyses and classifies the operation into known fault classes. Further, the variable perturbation module utilizes the diagnosis model specific to the corresponding fault class and identifies the most significant variables relevant to the fault. The outputs such as time of fault detection, the fault class and the most significant variables are conveyed to the operators of the industrial system for further analysis and taking appropriate corrective and preventive actions to mitigate the fault and its effects and to prevent failure of the industrial system.

In case false alarms, missed detections, misclassifications or previously unknown faults encountered by the fault detection and classification module, the operator can provide appropriate feedback such as correcting the label or assigning a new label to the identified fault. This feedback can be used to retrain the fault detection and classification model. Similarly, in case of an incorrect fault diagnosis, the operator can provide feedback by suggesting the correct set of most significant variables and their relative order of importance. This feedback can be used to retune the diagnosis model parameters. Period re-learning of the models based on operator feedback ensures the highest possible detection, classification, and diagnosis accuracies for the proposed system. The detailed description of each of the modules is presented below.

2.1. Fault Detection and Classification

The objective of fault detection and classification is to detect and classify the detected faulty operation into one or

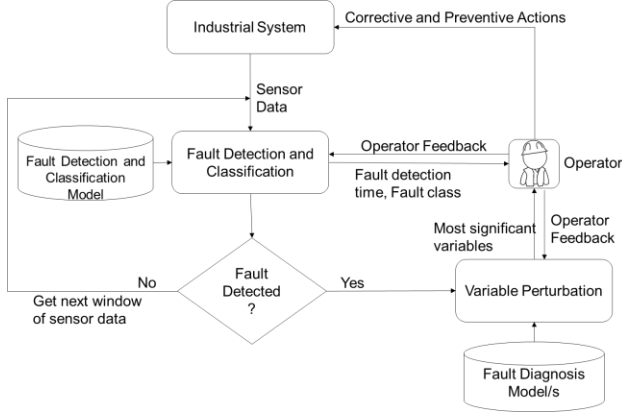


Figure 1. Proposed approach for fault diagnosis

more know fault types. In this work, the LSTM network is used for fault classification due to its capability in capturing long term temporal dependencies in time-sequence data (Hochreiter & Schmidhuber, 1997). In addition to the input provided via the input layer, LSTM uses previous hidden state information. In an LSTM cell, the flow of information is regulated using input (i), output (o) and forget (f) gates. The cell state c_t and hidden state h_t are computed in a recurrent manner as shown in Eq. (1).

$$\begin{aligned}
 f_t &= \sigma(W_f x_t + U_f h_{t-1} + b_f) \\
 i_t &= \sigma(W_i x_t + U_i h_{t-1} + b_i) \\
 o_t &= \sigma(W_o x_t + U_o h_{t-1} + b_o) \\
 \tilde{c}_t &= \tanh(W_c x_t + U_c h_{t-1} + b_c) \\
 c_t &= f_t \odot c_{t-1} + i_t \odot \tilde{c}_t \\
 h_t &= o_t \odot \tanh(c_t)
 \end{aligned} \tag{1}$$

Where x_t , h_t , and c_t are input, hidden and cell state vectors at time t , respectively. $\sigma(\cdot)$ and $\tanh(\cdot)$ are sigmoid and hyperbolic tangent activation functions. W and U are trainable weight parameters of the input and previous hidden connections and b are bias vectors respectively. The gradient descent method is used to determine the optimal values of trainable parameters for minimizing the categorical cross-entropy cost function shown in Eq. (2).

$$\mathcal{L}(y, \hat{y}) = \sum_{l=1}^C y_l \log \hat{y}_l \tag{2}$$

2.2. Variable Perturbation

If the fault is detected and identified, the next step is to identify the most significant variables responsible for the faulty operation. This is performed by the variable perturbation approach. The proposed fault localization approach utilizes multi-stage variable perturbation to identify the key variables relevant to the faulty operation. In

this method, the cumulative change in the score of the diagnosis models with respect to each feature is computed. The cumulative disturbance is obtained by summing the perturbation score from all iterations wherein in each iteration, the perturbation score is the output of the diagnosis model obtained by replacing the faulty data with the corresponding normal data of the feature in each diagnosis window. Figure 2 illustrates the approach for two iterations where D_{w^-} and D_{w^+} represent the diagnosis windows before and after the fault detection point respectively used for variable perturbation. In each iteration, the diagnosis windows on either side of the detection point are moved further away from the detection point as shown in Figure 2.

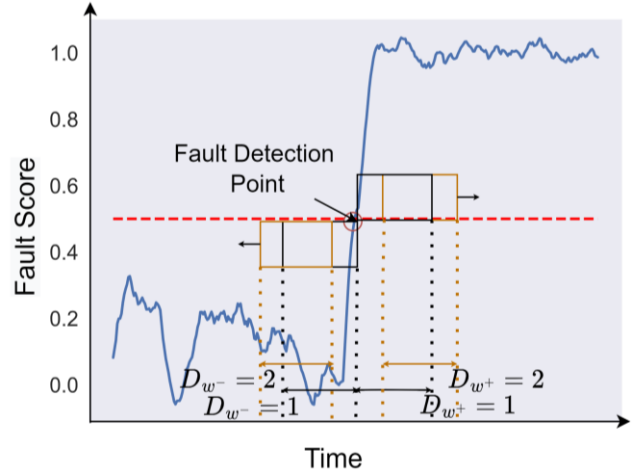


Figure 2. Multiwindow variable perturbation

The diagnosis model is trained to fit the fault score across the detection point and is specific to every fault class. It can be a data-driven model (regression model), mechanistic model or other functional approximation. The underlying assumption is that the fault score generated by the diagnosis model can be approximated as a sum of nonlinear functions of the process variables and tunable parameters. Mathematically, the fault score, s is approximated as,

$$\begin{aligned}
 s &= \sum_0^L f_L(x_i, x_j, x_k, \dots, \theta_l) \\
 &\forall L \in N \\
 &\& \forall i, j, k \in N
 \end{aligned} \tag{3}$$

Where, f_L is a nonlinear function, L is the number of nonlinear functions, θ_l are parameters of the function f_L , and x_i, x_j, x_k are the features/variables.

In this work, the fault score function is be approximated using multiple machine learning techniques such as Random Forest, XGBoost and LSTM. Assuming that a good diagnosis model that has learnt the above functional form and distinguishes faulty operation from normal operation across the detection point is available, the first order

variable perturbation matrix across the detection point can be calculated across diagnosis windows of equal length and summed as shown in Eq. (4).

$$J^1(i) = \sum_0^K \frac{\Delta s}{\Delta x_i} \quad (4)$$

$\forall i \in N,$

where K is the number of iterations for which perturbation is performed on either side of the fault detection point. Based on the perturbation score, the features are sorted and f_1 fraction of variables having a low perturbation score are rejected. The rest, i.e., $(1 - f_1)$ fraction of variables are used to calculate the second order variable perturbation matrix across the detection point over K number of diagnosis windows as shown in Eq. (5).

$$J^1(i, j) = \sum_0^K \frac{\Delta s}{\Delta x_i \Delta x_j} \quad (5)$$

$\forall i, j \in N,$

The absolute perturbation score of each feature in the second order perturbation matrix can be calculated by taking the mean around the second dimension (i.e., row mean) of the matrix. The features are sorted once again with respect to the absolute perturbation score and f_2 fraction of variables having low score are rejected and the rest $(1 - f_2)$ fraction of variables are carried forward. Now, the third order variable perturbation matrix is calculated over K diagnosis windows as shown in Eq. (6).

$$J^1(i, j, k) = \sum_0^K \frac{\Delta s}{\Delta x_i \Delta x_j \Delta x_k} \quad (6)$$

$\forall i, j, k \in N,$

Here, f_1, f_2, f_3 are the parameters of the approach.

The absolute perturbation score of each feature in the third order perturbation matrix can be calculated by taking the mean over the third dimension (matrix mean) of the matrix. The features are then sorted using the absolute perturbation score values. Similarly, higher order perturbation matrix calculations can be performed to arrive at a smaller number of remaining variables. However, it is observed that the third order perturbation with higher variables rejection rates is sufficient to reach a reasonable number (e.g., 5) of remaining variables.

Thus, using the variable perturbation matrix-based approach, one can arrive at the list of the most important variables having a dominant effect on the diagnosis model. These variables are considered to be the most significant variables relevant to the fault. Undoubtedly, the effectiveness of this approach depends on the efficacy of the diagnosis model in learning the distinction between faulty and normal operation. Development of accurate diagnosis models is, therefore, a crucial step in this approach.

3. SYSTEM DESCRIPTION

The utility of the approach is demonstrated on the industrial system presented in the 2021 Annual Data Challenge of the Prognostics and Health Management (PHM) Society, Europe which was sponsored by NVIDIA. The aim of the challenge was to have a fast and robust predictive maintenance solution for an industrial robotic test bed designed for quality control and assurance. Detecting and classifying the faults accurately and identifying the most significant variables of the faults in the lowest possible time were the key aspects of the challenge. The system of interest was provided by the Swiss Center for Electronic and Microtechnology (CSEM) and used for testing of fuses. The testing system mainly comprises a test bench for fuses and a 4-axis SCARA-robotic vacuum feeder arm to pick up the fuses. The fuse test bench further comprises two conveyor belts, an infrared thermal sensor set up and a robotic sorting bar. The test bed is shown in Figure 3 and the processing steps are described below:

1. First, fuses are picked and transported within the range of infrared sensor by the robotic feeder
2. Fuses are first tested for their conductivity and later for their quality by applying a 200 mA current for 1.5 sec and simultaneously measuring their responses
3. After the test, fuses are transported to the main conveyor belt for further sorting
4. Fuses are sorted by the robotic sorting bar based on their test results
5. These fuses are transported by the conveyor belt to the feeder
6. Finally, the fuses are transported by another conveyor belt to the next processing step such as labeling or packing

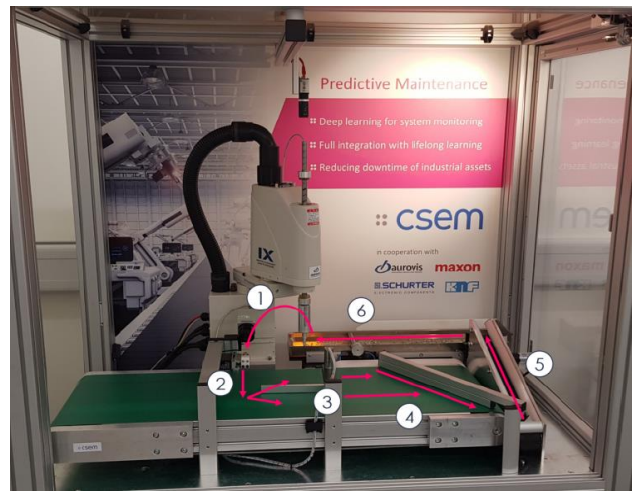


Figure 3. Industrial test bed set up (PHME-Data Challenge [2021])

The system is instrumented well to measure the state of its health, the surrounding environment, and other auxiliary

systems of the machine. A total of 50 variables related to the system health (pressure, vacuum etc.) and environment conditions (temperature, humidity, etc.) are monitored and their time series features are recorded at 10 sec time intervals. The time series features include the maximum value, minimum value, mean, frequency, total count, and trend of each variable.

Various faults such as conveyor failure due to motor fault or high frictional losses, pneumatics fuse feeder failure due to pressure leakage, robot gripper failure due to vacuum system fault, and other failures due to noisy measurement and desyncing of robotic feeder can occur in the test bed. A total of 6 faulty operating conditions are observed in the system. Accurate detection, classification, and diagnosis of these faults in the shortest possible time is of utmost importance to the test bed operator. This increases the productivity and efficacy of the testing process, minimizes the losses due to false positives, and reduces the unnecessary alarms and warnings thus reducing the cognitive load on the operators. Similarly, timely corrective actions will minimize the losses and reduce adverse impact on the health of the test bed.

4. MODEL DEVELOPMENT

The development of deep learning models for fault classification and fault diagnosis is discussed here. The initial dataset consisted of 50 variables, out of which 17 variables are omitted as they had no variability (zero standard deviation). The remaining 33 variables are considered for building the fault detection & classification, and diagnosis models.

4.1 Fault Detection and Classification Model

A LSTM classifier is trained for combined fault detection and classification. For training the model, a total of 57000 data points comprising normal instances as well as faulty instances of each fault class. 20% of the data is used as the test data for evaluating the model performance and the remaining 80% is used for training the network. The training data is first subjected to data pre-processing, where null values in the data are imputed using multivariate imputation, and the resultant data is normalized using z-score normalization.

The LSTM network comprises 2 hidden layers having tanh activation function followed by an output layer with single cell and sigmoid activation function. The number of cells in the hidden layer, the window size and the batch size are the hyper-parameters which are tuned using GridSearchCV during model training. The number of hidden cells is evaluated at values of 20, 50, 100 and 200. Considering the data size and dynamics of the system, window sizes are evaluated at values of 5, 10, 15 and 20, and the batch size is evaluated at values of 16, 32, 48 and 64. The model is trained for a maximum of 150 epochs. The categorical cross

entropy between actual and predicted labels is computed after each epoch and early stopping with a patience of 5 is used to prevent overfitting. The optimal values of hyper-parameters obtained for the trained model are 100 LSTM cells in both the hidden layers, a window size of 5 and a batch size of 16.

The confusion matrix obtained on the test data using the trained LSTM classifier for all fault classes is shown in Figure 4. An overall fault classification accuracy of 98.92 % is obtained.

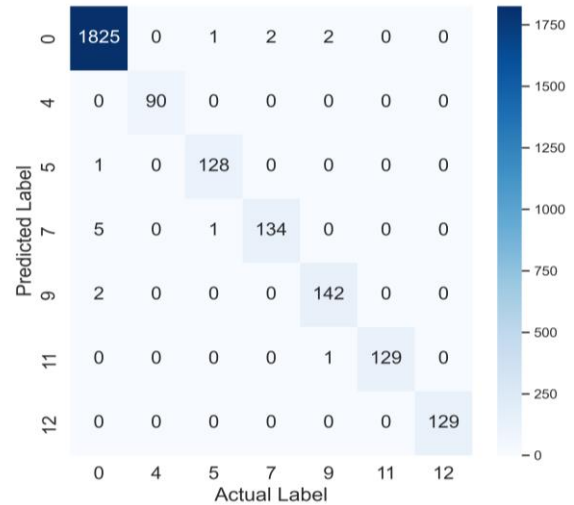


Figure 4. Confusion matrix for fault detection and classification model on the test data. Numbers in the confusion matrix are number of windows in the test data

4.2 Fault Diagnosis Model

For the fault diagnosis model, various ML techniques such as Random Forest and XGBoost, and DL techniques such as LSTM are experimented with. These techniques are shortlisted based on their capability to learn nonlinear behavior and sensitivity to faults. The diagnosis model is trained as regression model to fit the fault (probability) score from the fault detection & classification model around the detection point. Therefore, one diagnosis model is trained for each fault class.

For each fault class, multiple files of faulty operation data are provided. These are utilized for training and validating the diagnosis models. In each file, the initial portion consisted of data from normal operation of the test bed while the end portion consisted of data from faulty operation, and the transition point from normal to faulty operation was anywhere in the middle. The train-test split approach considered for the diagnosis models is different from the commonly used random split approach. 25 % of the instances from each extreme end of the data are selected for training and the points across the detection points are used for validation. Once the diagnosis models are built, their validation is done by applying the VPM approach on

the validation data. The most significant variables obtained from VPM are then compared with the ground truth variables available for each fault class. Validation is performed by ascertaining the consistency of the most significant variable groups identified for each fault class, reproducibility of the results on data files of the same fault class, and differences in the variables shortlisted across different fault classes.

Based on these validation criteria, LSTM diagnosis models were found to perform better than models built using other techniques, possibly due to better learning of the evolving fault signature. Thus, LSTM models are finalized for fault diagnosis using the VPM approach. For each fault class, a separate LSTM model is built for better specificity of the results. The ranges of optimal parameters of the LSTM models obtained after hyper-parameter tuning and the optimal VPM approach parameters, perturbation window length and rejection rate are tabulated in Table 1.

5. RESULTS AND DISCUSSION

The ground truth in terms of key variables pertaining to fault classes 4, 5, 7, 9, 11 and 12 in the test bed is provided by the organizers of the PHME-21 data challenge and is used to verify the effectiveness of the proposed approach. The trained LSTM model for fault detection and

Table 1. Optimized ranges of network parameters for the LSTM diagnosis models

Parameter	Optimal Value
Number of hidden layers	2
Number of cells	64 to 256
Batch size	32
Window size	15
Activation function	ReLU
Epochs	120
Rejection Rate (f_1, f_2, f_3)	0.5
Perturbation window length	8 to 10

classification is used to detect and classify the faults. The LSTM fault diagnosis model specific to the detected fault is then used to compute the cumulative perturbation score for each of the variables using the methodology described in Section 2.2. For each of the 6 fault classes, the variables are ranked in decreasing order of the cumulative score. The trend of cumulative perturbation score for the significant variables across the iterations for each fault class are shown in Figure 5. It can be observed that for almost all fault classes, the cumulative score trend for the most significant variables separates from that of the rest of the variables indicating the effect of dominant variables on the fault.

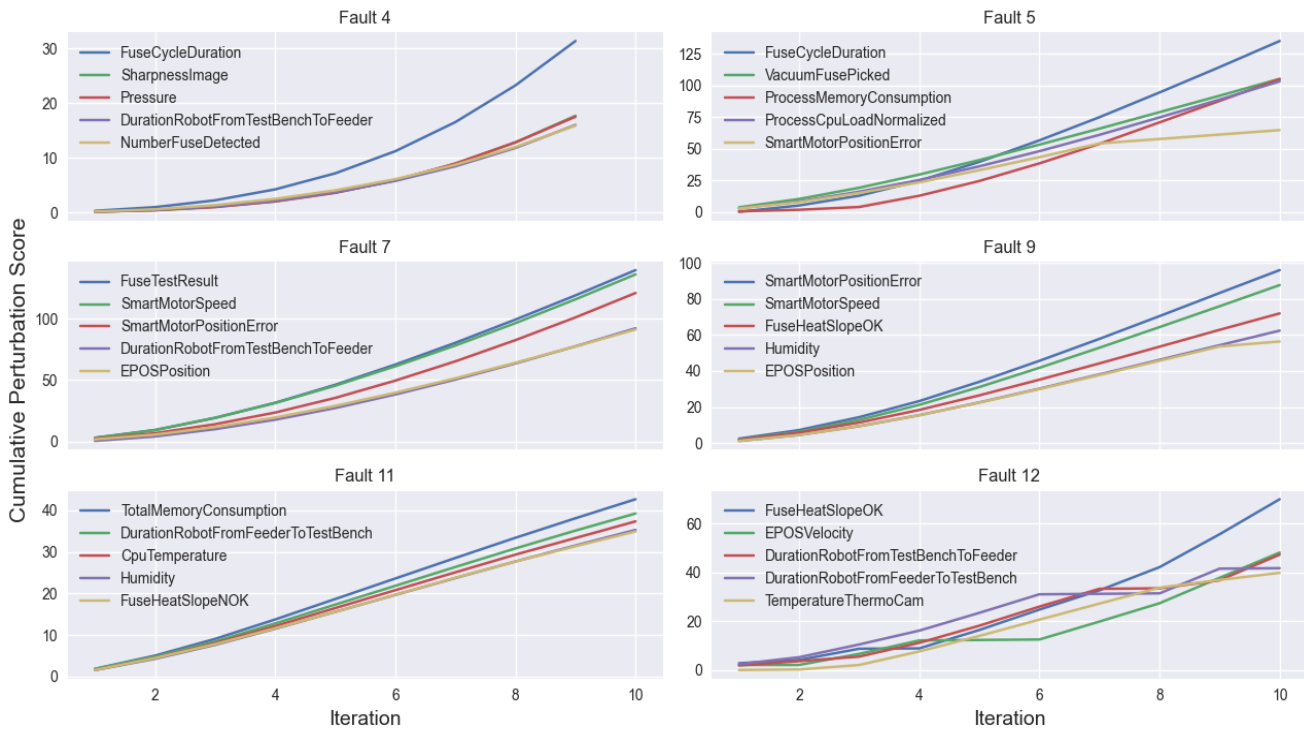


Figure 5. Cumulative perturbation score for all fault classes

Table 2. Most significant variables identified for each fault class

Fault Class	Ground Truth Variables	Most Significant Variables	Diagnosis Accuracy
4	Pressure	FuseCycleDuration SharpnessImage Pressure	0.7
5	VacuumFusePicked Vacuum	FuseCycleDuration VacuumFusePicked ProcessMemoryConsumption	0.85
7	VacuumFusePicked FusePicked	FuseTestResult SmartMotorSpeed SmartMotorPositionError	0.5
9	SmartMotorSpeed SmartMotorPositionError	SmartMotorPositionError SmartMotorSpeed FuseHeatSlopeOK	1
11	SmartMotorSpeed SmartMotorPositionError	TotalMemoryConsumption DurationRobotFromFeederToTestBench CpuTemperature	0.5
12	DurationRobotFromFeederToTestBench DurationRobotFromTestBenchToFeeder	FuseHeatSlopeOK EPOS Velocity DurationRobotFromFeederToTestBench DurationRobotFromTestBenchToFeeder	0.7

The top 3 most significant variables identified for each fault class are compared with the corresponding ground truth variables and are shown in Table 2. The diagnosis accuracy of the approach is computed using the most significant variables for each fault class as follows:

$$\text{Diagnosis Accuracy} = \begin{cases} 1 - 0.15(x - 1), & \text{if } x < 4 \\ 0.5, & \text{otherwise} \end{cases} \quad (7)$$

where, x is the position of the ground truth variable in the list of most significant variables. The diagnosis accuracy for each fault class is shown in Table 2.

Table 2 shows that the most significant variables are correctly diagnosed for faults 4, 5, 9 and 12 with a high degree of accuracy. For fault class 4, the ground truth variable, 'Pressure' is identified correctly by the approach as the third most significant variable for the fault. For fault class 5 too, the ground truth variable, 'VacuumFusePicked' is correctly identified along with two other variables 'FuseCycleDuration' and 'ProcessMemoryConsumption'. The ground truth variable is identified second in the order of significance. For fault class 9, there is a good match between the ground truth variables and the diagnosed variables. This is also clearly visible in **Error! Reference source not found.** where the cumulative score for 'SmartMotorPositionError' and 'SmartMotorSpeed' separated from the score of the rest of variables as the number of iterations increased. The identified variables

imply the error is caused due to variation in motor speed of conveyor belt. Similarly, for fault class 12, the ground truth variables match well with those identified by the approach. Figure 5 also shows that the signals representing robot arm duration, i.e., 'DurationRobotFromFeederToTestBench' and 'DurationRobotFromTestBenchToFeeder' had higher perturbation scores till iteration #6 indicating that the fault lies in the robot arm that is picking fuses from the feeder to the test bench and returning them after the test.

For fault class 7, however, the identified significant variables, 'FuseTestResult', 'SmartMotorSpeed' and 'SmartMotorPositionError' do not match directly with the ground truth variables i.e., 'VacuumFusePicked' or 'FusePicked'. For class 11 too, the ground truth variables i.e., 'SmartMotorSpeed' and 'SmartMotorPositionError' do not match with the diagnosed variables. In this case, however, the variable 'SmartMotorSpeed' is constant throughout the operation and therefore cannot be the correct ground truth variable for the fault. The most significant variables identified for this fault class are 'TotalMemoryConsumption', 'DurationRobotFromFeederToTestBench' and 'CpuTemperature'. These variables point to a possible fault in the robot arm causing an increasing load on the processor.

The average diagnosis accuracy for all fault classes combined is ~70.8% when the top 3 features are considered.

For only those fault classes where the significant variables are correctly identified, i.e., fault classes 4, 5, 9 and 12, the diagnosis accuracy is ~81.2%. The diagnosis accuracy from the proposed VPM approach is either on par or better than the diagnosis accuracies reported by the winners of the PHME-21 data challenge (80-82%) (Aydemir et al., 2021; Etxabe, Omella, & Perez, 2021).

6. CONCLUSION AND FUTURE WORK

In this work, a variable perturbation matrix-based approach for industrial fault diagnosis is proposed. The proposed approach utilizes a LSTM model for detection and classification of faults in the system and fault-specific LSTM diagnosis models to measure a multi-step cumulative perturbation score corresponding to each of the variables. The variables with the highest cumulative perturbation score are identified as the most significant variables related to the detected fault.

The approach is demonstrated on an industrial test bed for fuse testing whose operating data was provided for the PHME-21 Data Challenge. Out of 6 faults for which the ground truth is provided, the approach correctly identified the most significant variables for 4 fault classes with a diagnosis accuracy of ~81% and an overall diagnosis accuracy of ~71%. Reliable fault detection and diagnosis from the approach would help operators in reducing the time taken to address the faults thereby minimizing the impact of faults on the industrial system, and maintaining productivity, efficiency, and product quality.

Although the proposed approach is independent of the system and has produced fairly accurate results for the industrial test bed, its generalizability and effectiveness of fault localization for other systems, particularly systems having multiple components and significant process lags need to be investigated. Also, as the performance of the approach depends strongly on the underlying diagnosis model, more work is needed to establish the relation between different diagnosis model types and their corresponding diagnosis efficacies.

REFERENCES

- Aydemir, G., Avcı, A., Kocakulak, M., & Bekiryazıcı, T. (2021a). Ensemble of LSTM Networks for Fault Detection, Classification, and Root Cause Identification in Quality Control Line. *PHM Society European Conference*, 6(1), 6–6. <https://doi.org/10.36001/phme.2021.v6i1.3043>
- Aydemir, G., Avcı, A., Kocakulak, M., & Bekiryazıcı, T. (2021b). Ensemble of LSTM Networks for Fault Detection, Classification, and Root Cause Identification in Quality Control Line. *PHM Society European Conference*, 6(1), 6–6. <https://doi.org/10.36001/phme.2021.v6i1.3043>
- Belagoune, S., Bali, N., Bakdi, A., Baadji, B., & Atif, K. (2021). Deep learning through LSTM classification and regression for transmission line fault detection, diagnosis and location in large-scale multi-machine power systems. *Measurement*, 177, 109330. <https://doi.org/10.1016/j.measurement.2021.109330>
- Cho, S., Choi, M., Gao, Z., & Moan, T. (2021). Fault detection and diagnosis of a blade pitch system in a floating wind turbine based on Kalman filters and artificial neural networks. *Renewable Energy*, 169, 1–13. <https://doi.org/10.1016/j.renene.2020.12.116>
- Etxabe, K. L. de C., Omella, M. G., & Perez, E. G. (2021). Divide, Propagate and Conquer: Splitting a Complex Diagnosis Problem for Early Detection of Faults in a Manufacturing Production Line. *PHM Society European Conference*, 6(1), 9–9. <https://doi.org/10.36001/phme.2021.v6i1.3039>
- Fagarasan, I., & Iliescu, S. S. (2008). Applications of fault detection methods to industrial processes. *Undefined*. Retrieved from <https://www.semanticscholar.org/paper/Applications-of-fault-detection-methods-to-Fagarasan-Iliescu/1d8cc8ed6e91e6e3da3af568c0e07753864e75a9>
- Hochreiter, S., & Schmidhuber, J. (1997). Long Short-Term Memory. *Neural Computation*, 9(8), 1735–1780. <https://doi.org/10.1162/neco.1997.9.8.1735>
- Khoukhi, A., & Khalid, M. H. (2015). Hybrid computing techniques for fault detection and isolation, a review. *Computers & Electrical Engineering*, 43, 17–32. <https://doi.org/10.1016/j.compeleceng.2014.12.015>
- Kim, E., Cho, S., Lee, B., & Cho, M. (2019). Fault Detection and Diagnosis Using Self-Attentive Convolutional Neural Networks for Variable-Length Sensor Data in Semiconductor Manufacturing. *IEEE Transactions on Semiconductor Manufacturing*, 32(3), 302–309. <https://doi.org/10.1109/TSM.2019.2917521>
- Lee, G., Han, C., & Yoon, E. S. (2004). Multiple-Fault Diagnosis of the Tennessee Eastman Process Based on System Decomposition and Dynamic PLS. *Industrial & Engineering Chemistry Research*, 43(25), 8037–8048. <https://doi.org/10.1021/ie049624u>
- Li, C., Wei, F., Wang, C., & Zhou, S. (2017). Fault diagnosis and prediction of complex system based on Hidden Markov model. *Journal of Intelligent & Fuzzy Systems*, 33(5), 2937–2944. <https://doi.org/10.3233/JIFS-169344>
- Long, J., Mou, J., Zhang, L., Zhang, S., & Li, C. (2021). Attitude data-based deep hybrid learning architecture for intelligent fault diagnosis of multi-joint industrial robots. *Journal of Manufacturing Systems*, 61, 736–745. <https://doi.org/10.1016/j.jmsy.2020.08.010>
- Michau, G., Palm, T., & Fink, O. (2017). Deep Feature Learning Network for Fault Detection and Isolation. *Annual Conference of the PHM Society*, 9(1). <https://doi.org/10.36001/phmconf.2017.v9i1.2380>
- Park, P., Marco, P. D., Shin, H., & Bang, J. (2019). Fault Detection and Diagnosis Using Combined Autoencoder

- and Long Short-Term Memory Network. *Sensors*, 19(21), 4612. <https://doi.org/10.3390/s19214612>
- PHME-Datachallenge. (2022). *Data Challenge: 2021*. Retrieved from <https://github.com/PHME-Datachallenge/Data-Challenge-2021> (Original work published 2021)
- Zhang, W., Yang, D., & Wang, H. (2019). Data-Driven Methods for Predictive Maintenance of Industrial Equipment: A Survey. *IEEE Systems Journal*, 13(3), 2213–2227. <https://doi.org/10.1109/JSYST.2019.2905565>
- Zhang, Y.-W., & Qin, S. J. (2010). Decentralized Fault Diagnosis of Large-scale Processes Using Multiblock Kernel Principal Component Analysis: Decentralized Fault Diagnosis of Large-scale Processes Using Multiblock Kernel Principal Component Analysis. *Acta Automatica Sinica*, 36(4), 593–597. <https://doi.org/10.3724/SP.J.1004.2010.00593>